



# Assessment of pyrolysis waste engine oil as an alternative fuel source for diesel engine

A. Zahir Hussain<sup>1</sup> · A. Santhoshkumar<sup>1</sup> · Anand Ramanathan<sup>1</sup>

Received: 9 November 2019 / Accepted: 5 March 2020 / Published online: 17 March 2020  
© Akadémiai Kiadó, Budapest, Hungary 2020

## Abstract

Disposal of hazardous waste engine oil (WEO) has become the forefront of climate change. Hence, the potential conversion of WEO is essential and also recycled through different pyrolysis techniques for better assessment. In this work, diesel-like fuel extracted from electrical pyrolysis and microwave pyrolysis was used as an alternative fuel for the CI engine. The pyrolysis oil generated by both pyrolysis processes was found to be reliable. Nevertheless, the physicochemical characteristics of both pyrolysis oil deviated from each other. The performance, combustion and emission characteristics of different pyrolysis fuel have been investigated to identify the suitable alternative fuel for CI engine. The performance characteristics at rated load revealed that the brake thermal efficiency of electrical pyrolysis oil (EPO) and microwave pyrolysis oil (MPO) was 26% and 25%, respectively, which was 0.8% and 1.5% lower than diesel due to its higher viscosity. Emission characteristic shows that unburnt hydrocarbon emission of EPO and MPO was higher than diesel by 7% and 15%, respectively. Similarly, the filter smoke number was 3% and 10% higher than diesel. NO emission of EPO and MPO was lower than diesel by 27% and 13%, respectively. Also, exergy analysis represents MPO has higher potential when compared to EPO due to higher exergy efficiency.

**Keywords** Waste to energy · Pyrolysis · Performances · Emissions · Exergy

## Abbreviations

AC	Activated carbon	NCG	Non-condensable gases
ASTM	American Society for Testing and Materials	NO	Nitric oxide/ppm
BTE	Brake thermal efficiency/%	NO <sub>x</sub>	Oxides of nitrogen/ppm
BMEP	Brake mean effective pressure/bar	PAHs	Polycyclic aromatic hydrocarbons
BSEC	Brake specific energy consumption/MJ kWh <sup>-1</sup>	ppm	Parts per million
CA	Crank angle/degree	PO	Pyrolysis oil
CI	Compression ignition	UBHC	Unburnt hydrocarbon/ppm
CO	Carbon monoxide/vol%	WEO	Waste engine oil
CO <sub>2</sub>	Carbon dioxide/vol%		
DI	Direct injection		
EPO	Electrical pyrolysis oil		
FEO	Fresh engine oil		
FSN	Filter smoke number		
GC–MS	Gas chromatography and mass spectrometry		
HRR	Heat release rate/J deg <sup>-1</sup> CA <sup>-1</sup>		
MAP	Microwave-assisted pyrolysis		
MPO	Microwave pyrolysis oil		

## Introduction

Waste management and waste treatment are one of the essential concerns of modern civilisation as it is challenging to find a collective treatment for them [1]. Most of the wastes are problematic to recycle, and huge amounts of landfilled waste resources are presented throughout the world. Disposal of hazardous wastes creates pollution issues and greenhouse gas emissions without the retrieval of toxic components [2]. Waste disposals such as spent engine oil, biomass, non-recyclable plastics and waste tires cannot be used as a combustible fuel until it can be refined [3]. The waste oil contains a higher amount of unwanted environment pollutants such as

✉ Anand Ramanathan  
anandachu@nitt.edu

<sup>1</sup> Department of Mechanical Engineering, National Institute of Technology, Tiruchirappalli, TamilNadu 620 015, India

PAH, heavy metals (copper, lead, iron, etc.) and sulphur [4]. Also, those wastes have several harmful effects on human beings and the environment. Around the world, more than 60% of the used lubricant oil is disposed of as waste. Every year, around 40 million metric tons of waste lubricant oils are generated [5]. In addition, the steady increase in the number of diesel vehicles on the road creates the two major problems of conventional fuel decrement and environmental pollution from toxic emissions [6]. Moreover, the fast depletion of fossil fuel resources and limited conventional fuel reserve has led to an intensive search for alternate fuel for a diesel engine; also, the alternative fuel derived from renewable and non-renewable waste can maintain the same engine performance and emission characteristics as that of diesel, which is gaining attention [7]. Therefore, this is an excellent initiative for deriving alternative energy from the waste products which serves the dual purpose of alternative energy source and waste management [8].

Pyrolysis is a familiar thermochemical approach to obtain valuable products such as diesel-like fuels from waste oils [9], plastics [10] and biomass residues [11]. The final gas, liquid and solid products derived from the pyrolysis process and these yields will vary depending on the reaction parameters [12]. Generally, increasing the operating temperature of the pyrolysis process decreases the char yield and increases the gas yield [13]. Tripathi et al. investigated the pyrolysis of waste oil conducted at 300–800 °C, and their work reported a higher amount of saturated hydrocarbons formed at the temperature range of 350–400 °C [14]. The pyrolysis temperature at 350–400 °C is the preeminent technology for converting heavy metal-polluted waste into the most valuable products [15]. Lam et al. [16] investigated the pyrolysis of waste engine oil using metallic char catalyst. The presence of metal acts as a catalyst to increase the heterogeneous reaction like methane decomposition and attain the required temperature quickly. Moreover, the metal gets converted into metal oxides and absorbs the sulphur existing in the oil. The high volatile material Cd and Cr would be possible to vaporise at the pyrolysis temperature that exists above 400 °C [4].

Microwave-assisted pyrolysis (MAP) has several advantages over conventional pyrolysis which attracts the research society [17]. Microwave pyrolysis provides equal distribution of heat, efficient heat transfer, and then the heating methods of microwave pyrolysis can be controlled easily [18]. Microwave pyrolysis comprises an atypical heat transfer mechanism to the pyrolysis feed through a microwave fascinating susceptor [19]. The microwave-assisted pyrolysis is much faster and energy efficient as compared to electrical heating due to localised heat generation and uniform volumetric heating of the feed [20]. In recent days, microwave-absorbing materials are becoming more popular to enhance the heating rate. Lam et al. [21] investigated the conversion of used frying oil into biofuel products through

microwave pyrolysis technique by contacting a bed of microwave absorbents such as particulate carbon, activated carbon and mesoporous aluminosilicate to increase the efficiency of the microwave pyrolysis process. Suriapparao et al. [22] investigated with silicon carbide, activated carbon and fly ash have used as susceptors in microwave pyrolysis of polypropylene, and the liquid yield percentages are 32%, 29% and 21%, respectively. Salema and Ani conducted microwave pyrolysis of oil palm shell with the addition of different mass ratios of activated carbon at input powers of 180 W and 450 W. It was observed that no pyrolysis takes place without the addition of susceptor [23]. Anand et al. [24] reported that 40% activated carbon required to increase the pyrolysis temperature and decrease the specific energy consumption of microwave pyrolysis. Hence, further investigation is required for the microwave pyrolysis and its fuel quality compared to conventional pyrolysis techniques.

Diesel engines are preferred prime movers for the transportation and agricultural sector due to their higher brake thermal efficiency, higher torque and less fuel consumption. Also, the diesel engine released higher carbon dioxide (CO<sub>2</sub>) emission when using high-viscous fuel which causes global warming emission. Hence, to reduce the carbon footprint is essential as per the Paris agreement so that the average earth temperature does not rise above 2 °C [25]. Also, high-viscous alternate fuel derived from organic and inorganic waste reduces the overall harmful emissions such as CO and NO<sub>x</sub> compared to petrol and diesel [26]. Thus, pyrolysis fuel obtained from the waste can be used as an alternative fuel for the diesel engine [27]. Several research works have been conducted on the utilisation of different high-viscous fuel in CI engine with fuel modifications and recognised the reliable operations [28]. The related literature is detailed in Table 1 [29] for the utilisation of high-viscous fuel blended with diesel [30]. Also, in recent days, experiments have exposed that the utilisation of pyrolysis fuel derived from surplus lubrication oil may be used as a substitute fuel for diesel [31]. Beg et al. [32], collected the purified oil from the shipyard then mixed with diesel at numerous quantities, and the fuel characterisations of all blends are determined. The blend of 35% treated oil had properties comparable to that of diesel. Arpa et al. [33] exposed diesel-like fuel derived from waste engine oil can be directly used as an alternative fuel for a diesel engine and also observes the stable engine operation without any difficulties. In another experimental study, the diesel-like fuel derived from surplus engine oil is mixed with turpentine with different blend ratios of 10%, 20% and 30%. The diesel-like fuel increases torque, brake thermal efficiency, mean effective pressure and drop in specific fuel consumption of CI engine for complete operation [34]. Murugan et al. [35] studied the performance, combustion and emission analysis of diesel engines using a different blend of distilled tire pyrolysis oil. They reported that the brake thermal efficiency

**Table 1** List of literature related with fuel modification for the high-viscous fuel

Sl. no	References	Fuel type	Performance characteristics		Emission characteristics			
			BTE	BSFC	CO	UBHC	NO <sub>x</sub> /NO	Smoke
1	Vedharaj et al. (Kapok Methyl Ester) [29]	Diesel	Base line fuel	Base line fuel	Base line fuel	Base line fuel	Base line fuel	Base line fuel
		B25	↑	↑	↑	↑	↑	↑
		B25 + 1,4-dioxane	↑	↓	↓	↓	↓	↓
2	Vigneswaran et al. [28]	Diesel	Base line fuel	Base line fuel	Base line fuel	Base line fuel	Base line fuel	Base line fuel
		Diesel + water + surfactant	↑	↑	↓	↓	↓	↓
		Diesel + water + surfactant + 1,4 dioxane	↑	↑	↓	↓	↓	↓
3	Nanthagopal et al. (calophyllum inophyllum biodiesel) [30]	Diesel	Base line fuel	Base line fuel	Base line fuel	Base line fuel	Base line fuel	Base line fuel
		B50	↓	↑	↓	↓	↑	↓
		D50 + B50 + 10% diethyl ether	↓	↓	↓	↓	↓	Similar to diesel

of the engine increases with the blend percentage but always is less than that of clean diesel. Also, the pyrolysis oil blends lowered the NO emission and increased the UBHC emission when compared with clean diesel [36].

In an overview of the primary literature, the pyrolysis of waste engine oil is a promising technology to reduce the carbon footprint. Also, diesel-like fuel can be extracted from a different kind of pyrolysis process. Among that, microwave pyrolysis is an energy-efficient technology for extracting high value-added products from the waste engine oil with a lower carbon footprint. An earlier study has been reported that the pyrolysis of waste engine oil was carried out on the electrical pyrolysis and microwave pyrolysis reactor. The properties of electrical pyrolysis oil were superior to microwave pyrolysis. However, microwave pyrolysis became energy efficient and increased research attention [3]. Although, the previous study was carried out on a different scale of electrical and microwave pyrolysis processes. Therefore, further investigation is required to identify the pyrolysis fuel properties in electrical pyrolysis and microwave pyrolysis on the same scale reactor. In the present investigation, the same quantity of feed was taken in both the electrical and microwave pyrolysis processes to assess the physicochemical characteristics. In addition to property analysis, these works are extended to the analysis of different pyrolysis WEO fuel's performance, combustion and emission characteristics on the CI engine in the same environmental conditions to identify the suitable alternative fuel and its potential capabilities. This work is mainly concentrated on how the fuel properties are influenced by the CI engine combustion even though fuel derived from the same feed source. For the first time, the comparative analysis of electrical and microwave pyrolysis oils was tried as sole fuel in a conventional diesel engine as an alternative

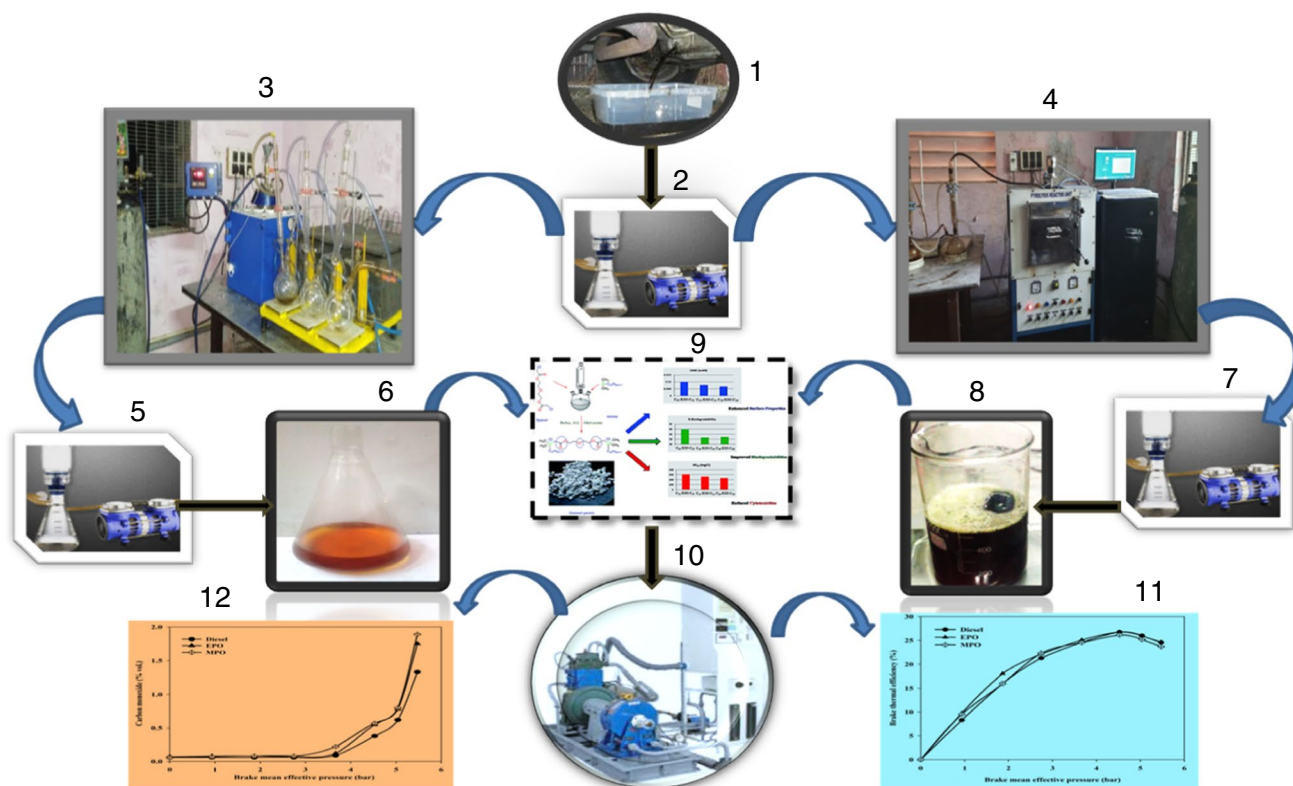
fuel. Few works have also been reported by using pyrolysis fuel as a sole fuel in a diesel engine. An overview of the literature, the alternative fuels were mixed with diesel and additives were added to improve the performance and reduce the engine emissions. Hence, the initial phase of the work started with electrical and microwave pyrolysis oil production; also, the work extended to performance and emission characteristics of pyrolysis oil in a CI engine were analysed without any engine and fuel modification. Also, the exergy analysis of different fuels has been carried out to identify the fuel potential.

## Pyrolysis process

The earlier work reported that the difference between the physicochemical properties of electrical and microwave pyrolysis oils [3]. Continuation of our previous work, this work compares the properties of electrical and microwave pyrolysis oils carried out on the same scale reactor. In our earlier work, the different quantity of feed was taken in both electrical and microwave pyrolysis. However, in present work, an equal amount of feed was taken, and the difference between the physicochemical properties of electrical and microwave pyrolysis oil has been found to improve the findings. The detailed experimental procedure and each step involved in this study are given below. The outline and methodology of the proposed work are given in Fig. 1.

## Pre-treatment of waste engine oil

Waste engine oil (WEO) collected from various automobile service stations was stored in a conventional common



1. Waste engine oil collection
2. Removal of heavy metal contaminants
3. Electrical pyrolysis
4. Microwave pyrolysis
5. Purification of electrical pyrolysis oil (EPO)
6. Purified EPO
7. Purification of Microwave pyrolysis oil (MPO)
8. Purified MPO
9. Characterisation of EPO and MPO
10. Engine study using EPO and MPO
11. Performance characteristics
12. Emission characteristics

**Fig. 1** Outline of the proposed work

storage tank. The WEO was filtered through a  $< 100 \mu\text{m}$  membrane filter to remove heavy metal contaminants of size more than  $100 \mu\text{m}$ . After completing the pre-treatment, WEO was stored in a separate collection tank to maintain the homogeneity of the WEO before the pyrolysis process.

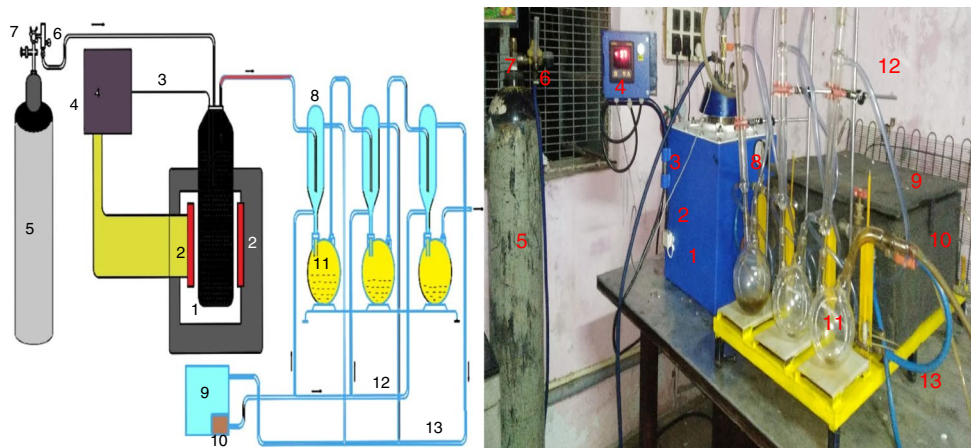
### Electrical pyrolysis set-up and configuration

Figure 2 represents the schematic and photographic view of an electrical pyrolysis reactor and its accessories. The electrical pyrolysis was carried out in a cylindrical stainless steel reactor with a maximum power of 3 kW. The industrial resistive type box heater was converted into an electrical

pyrolysis reactor. The 1.2 L of waste engine oil was precisely measured, and it has taken in 1.5 L of cylindrical stainless steel reactor. The pyrolysis temperature was maintained between 350 and 400 °C, and the heating rate was set to  $5 \text{ }^\circ\text{C min}^{-1}$ . The pyrolysis temperature range was fixed between 350 and 400 °C based on the TGA result reported on earlier research [3]. The temperature was measured using a K-type thermocouple connected with SELEC TC303 controlling unit. The power supplied to the reactor was cut off after reaching the desired temperature. The outer wall of the heater has been covered by glass wool and ceramic bricks to avoid the heat transfer between the reactor and the surroundings.



**Fig. 2** Schematic and photographic view of electrical pyrolysis reactor



- |                       |                                    |                             |
|-----------------------|------------------------------------|-----------------------------|
| 1. Electrical reactor | 2. 3 kW resistive heaters          | 3. K type thermocouple      |
| 4. Microcontroller    | 5. N <sub>2</sub> storage cylinder | 6. N <sub>2</sub> rotameter |
| 7. Flow controller    | 8. Liebig Condenser                | 9. Water tank               |
| 10. Circulating pump  | 11. Collecting flask               | 12. Water to condenser      |
| 13. Water to tank     |                                    |                             |

**Microwave-assisted pyrolysis set-up and configuration**

Figure 3 shows the photographic view of a microwave-assisted pyrolysis set-up. Schematic view and experimental procedure of microwave-assisted pyrolysis (MAP) was explained in earlier research [37]; the activated carbon (AC) was used as the microwave susceptor to increase the process efficiency [23]. Our previous work reports that the addition of AC decreased the specific energy

consumption and increased energy recovery of the process [38]. Figure 2 is the schematic view of the MAP reactor with accessories. The MAP reactor was operated at a frequency of 2.45 GHz and could increase the temperature up to 1000 °C. The MAP set-up consists of four 1.1 kW magnetrons placed opposite as a pair to ensure uniform heat generation. The reactor power was maintained at 1.1 kW and 2.2 kW by adjusting active magnetrons. The sequential switching of the active magnetron in every 3 min was followed to control overheating. In a 1.1 kW power supply, only one magnetron was used at a time. However, for the 2.2 kW power supply, two magnetrons were used. To prevent overheating of the magnetrons, a protective ventilation system was used to remove excess heat. During all MAP trials, 1.2 L of WEO was mixed with activated carbon (AC) and the mass ratio of AC was maintained at 30–40% to facilitate the energy conversion. The WEO and AC mixture was precisely weighed and taken in 1.8 L quartz vessel. Quartz has been chosen as a reactor vessel due to excellent microwave transparent property and withstands the higher temperature during the pyrolysis process. The temperature of the MAP was maintained between 350 and 400 °C, where the same K-type thermocouple was used to measure the temperature. Power consumption and temperature of the reactor were recorded using the Erotherm data acquisition system.



- |                             |                            |                  |
|-----------------------------|----------------------------|------------------|
| 1. Nitrogen cylinder        | 2. Data acquisition system | 3. Magnetron     |
| 4. Blower                   | 5. Quartz vessel           | 6. Stirrer motor |
| 7. Control panel            | 8. Water tank with pump    | 9. Condenser     |
| 10. Nitrogen flow regulator |                            |                  |

**Fig. 3** Schematic and photographic view of microwave pyrolysis set-up

**Nitrogen supply and after treatment of condensate**

To maintain the inert atmosphere inside the reactor, a nitrogen flow rate of 2–5 L min<sup>-1</sup> was maintained during the pyrolysis process. Pyrolysis gas from the reactor was

condensed in a Liebig water-cooled condenser. The cooling water at ambient temperature was used to condense the gas and collected in a collection jar. Non-condensable gas was purged through the water to remove soot and particulate matters. The condensate was then filtered using a 0.45  $\mu\text{m}$  membrane filter for further investigation.

### Comparison of pyrolysis yield for electrical and microwave pyrolysis

The disparity of pyrolysis yield for both electrical pyrolysis and microwave pyrolysis was reported in our previous research [3]. From the continuation of that work, the pyrolysis yields have been verified on the same scale reactor to find a suitable method for the waste engine oil pyrolysis. The maximum pyrolysis oil yield of 78% was obtained in the electrical pyrolysis, which is 6% higher than microwave pyrolysis. Also, pyrolysis yield was 4% higher than the small-scale reactor which is mentioned in our previous publication [3]. Higher localised heat generation and faster heating rate of microwave pyrolysis promote the secondary reaction, and C–C fission causes lower pyrolysis yield. Increase in the scale of the electrical pyrolysis decreased the surface evaporation and secondary cracking on the surface which influences the higher pyrolysis yield. The non-condensable gas yield was noticed higher in microwave pyrolysis due to secondary cracking caused by the localised heat generation. Moreover, char yield was decreased in the microwave pyrolysis due to localised temperature and carbon evaporation in the microwave field. The maximum non-condensable yield of 18% was noticed in the microwave pyrolysis, which is 10% lower than electrical pyrolysis. Similarly, char yield was 10% in microwave pyrolysis, which is 4% lower than electrical pyrolysis.

## Characterisation and analytical method

### Properties of pyrolysis engine oil

Table 2 shows the physicochemical properties of the pyrolysis oil obtained from both electrical pyrolysis and microwave pyrolysis as per the ASTM standards. The density and kinematic viscosity of MPO higher than electrical pyrolysis due to localised heat generation and faster heating rate cause wax

**Table 3** Elemental analysis of diesel, EPO and MPO

Elemental analysis/% in mass	Diesel fuel	EPO	MPO
C%	85.74	82.34	81.45
H%	13.72	14.67	17.34
N%	0.483	1.01	0.731
S%	0.0489	1.98	0.48

**Table 4** GC-MS analysis of EPO and MPO

Hydrocarbon groups	EPO	MPO
Alkanes %	75.5800	73.9100
Alkenes %	22.9600	14.8900
Cycloalkanes %	0.6500	0.4000
Alcohol %	0.0000	1.6200
Others %	0.0000	9.1900

and heavier hydrocarbon evaporation. The calorific value of microwave pyrolysis slightly higher than electrical pyrolysis due to short-chain hydrocarbon present in the fuel. Similarly, Tables 3 and 4 [3] report that elemental composition and GC–MS results for both electrical and microwave pyrolysis oil. The inference from the GC–MS results is that MPO contains slightly lower alkanes and alkenes when compared to EPO. Also, MPO contains 1.6% alcohol and 9.19% other constituents due to unpredictable reactions in the microwave pyrolysis reactor. The earlier work was already proved that hydrocarbon formation in the electrical and microwave pyrolysis [3].

### FTIR analysis for EPO and MPO

Figures 4 and 5 show the infrared spectrum of the EPO and MPO through FTIR analysis. The general grouping of chemical compounds was identified from the FTIR spectrum, with the help of the degree of infrared absorptions (or transmittance). The different frequencies detected through FTIR for the test fuels EPO and MPO are given in Table 5. A small difference in the frequency for EPO and MPO samples were noticed from FTIR spectra, and a small difference in the transmittance peak concentrations was also seen at a wide range of frequencies. The result shows that most of the HC found in oils were

**Table 2** Properties of diesel, EPO and MPO

Property	Diesel	EPO	MPO	ASTM standards
Density/kg m <sup>-3</sup> at 40 °C	828.1	842	855	ASTM 1298
Kinematic viscosity/cSt at 40 °C	2.417	2.98	5.24	ASTM D445
Low calorific value/kJ kg <sup>-1</sup>	42,110	42,920	44,210	ASTM D240
Copper strip corrosion	1a	1b	1b	ASTM D130
Carbon residue	0.002	0.002	0.004	ASTM D524

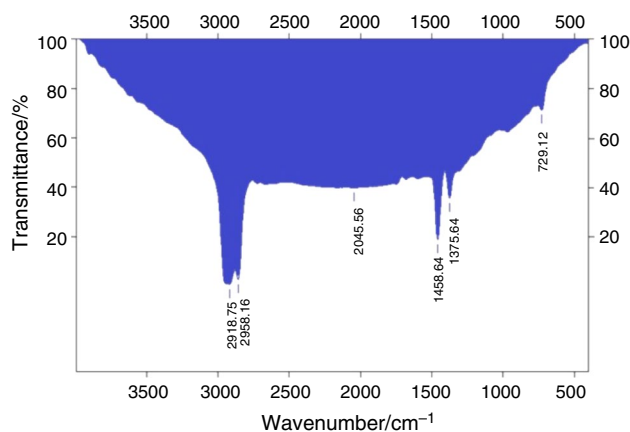


Fig. 4 FTIR result for EPO

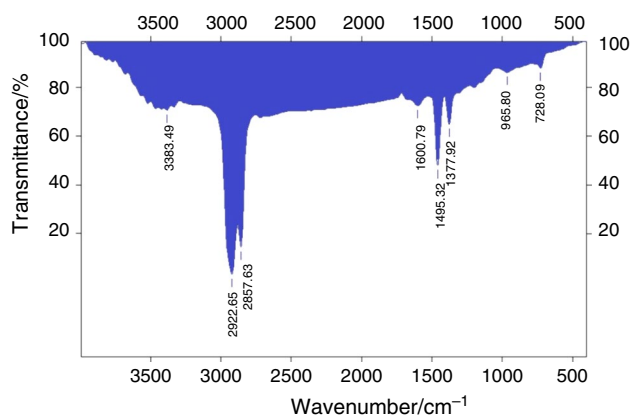


Fig. 5 FTIR result for MPO

carboxylic acids, alkenes, alkanes and single ring aromatics. EPO and MPO compounds with O–H, C=O, C–C, C–H and C=H widening vibrations like phenols, alkenes, aldehydes and single aromatics displayed very low peak intensities indicating the minor concentration of the compounds. However, low characteristic peaks of compounds were detected in the FTIR spectrum while measuring the scope of oxidation.

The admixture of oxygen to base oil molecules gives rise to oil oxidation, which results in the oxygenated by-product

formation along with hydroxyl (O–H) and carbonyl groups (C=O) like aldehydes and carboxylic acids. Carboxylic acids are unacceptable, which leads to the acidic corrosion and formation of sludge and formation of larger molecular species due to polymerisation of carboxylic acids. It can be resulted in increased oil viscosity and causing difficulties like filter persevering and system failure. The fundamental analysis showed that the presence of the major amount of oxygenated compounds in the pyrolysis oil causes the small quantity of oil oxidation and leads to low oxygen fillings in the pyrolysis process as given in Table 5.

## Experimental

The engine study was performed under different loading conditions at a fixed speed of 1500 rpm on a four-stroke, single-cylinder, direct-injected, naturally aspirated 3.7 kW diesel engine. The engine was operated using diesel, EPO and MPO at 200 bar injection pressure. The engine load was varied from 0 to 110% using eddy current dynamometer. The eddy current dynamometer was coupled with engine set-up to measure the power and to adjust the load. The dynamometer arm was mechanically connected with a load cell that intern transmits an output signal corresponding to the applied load.

The technical specifications of the experimental engine are mentioned in Table 6, and a schematic diagram of the engine test set-up is depicted in Fig. 6. K-type thermocouples were connected with the test engine to measure the temperature at various locations. For the combustion studies, the KISTLER quartz pressure sensor and a crank angle encoder were provided. The received output impulses from the sensors were interfaced with a computer for displaying the engine out data. The received values were averaged for 40 consecutive cycles to avoid cyclic variation. The engine output data are fully configurable so that it is easy to obtain the variation of pressure with crank angle and pressure–volume diagram under several engine operational conditions. The display unit indicated engine load, engine speed, temperatures, the mass flow rate of fuel and mass flow rate of air at required points. The inherent software in the system estimated indicates power, brake

**Table 5** Functional Groups detected in WEO and PWE0

Frequency range/cm <sup>-1</sup>	Functional groups	Classification of compounds
(a) 3200–3400	O–H stretching	Alcohols, phenols or carboxylic acid
(b) 2750–3000	C–H stretching	Alkanes
(c) 1700–2100	C=O stretching	Aldehydes, ketones or carboxylic acid
(d) 1575–1675	C=C stretching	Alkenes
(e) 1345–1500	C–H bending/deformation	Alkanes
(f) 900–1200	C–H bending	Alkenes
(g) 675–850	C–H out of plane bending	Single ring aromatics

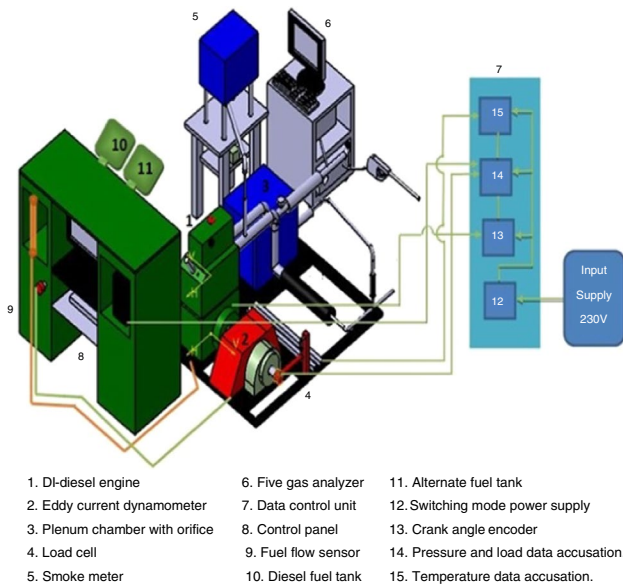
**Table 6** Specifications of the experimental engine

Engine parameter	Specification
Brand	TV1-KIRLOSKAR
Maximum power output	3.7 kW
Rated speed	1500 rpm
Cylinder	Single
Cooling type	Forced water circulation
Bore	80 mm
Stroke length	110 mm
Compression ratio	16.5:1
Fuel injection	Jerk type fuel injection (mechanical injection)
Operating pressure of the nozzle	200 bar
Fuel injection timing	23°bTDC

analysis was essential to prove the limits of accuracy of the experiments. The percentage of uncertainties and errors in the measuring parameters are determined by the ISO/IEC 17025 standards and National Accreditation Board for Testing and Calibration Laboratories (NABL 141) method. The uncertainty of these experiments is calculated based on the “Evaluation of Measurement data—Guide to the Expression of Uncertainty in Measurement” (GUM) approach. The expanded uncertainty of the experiment calculated with accounting repeatability, accuracy, resolution, precision and coverage factor. As per the GUM approach, normal distribution was selected for the resolution and rectangle distribution with a 95% confidence band was chosen for accuracy and range to find the maximum uncertainty of the experiment. Equations (1) and (2) show the combined and expanded uncertainty of this experimental work.

$$U_{\text{Combined}} = \sqrt{(U_{\text{repeatability}})^2 + (U_{\text{accuracy}})^2 + (U_{\text{resolution}})^2 + (U_{\text{precision}})^2 + (U_{\text{calibration}})^2} \quad (1)$$

$$U_{\text{expanded}} = \frac{U_{\text{Combined}}}{2} \quad (2)$$

**Fig. 6** Schematic diagram of experimental engine set-up

power, BSFC, volumetric efficiency and thermal efficiency. The engine exhaust gas constituents were analysed using AVL DiTestgas 1000 BL five gas analyser. The exhaust smoke emission was measured by using AVL 415SE smoke meter.

## Uncertainty analysis of engine parameters

Uncertainty and error in this present investigation may arise from the selection of tool, calibration, working conditions, working environment, the procedure for the conduct of the tests and observation. Uncertainty and error

where  $U$  is the uncertainty of depended parameter.

The accuracy and uncertainty of the measuring instruments are detailed in Table 7. The summaries of expanded uncertainties in absolute and percentage values of engine performance and emission parameters are given in Table 8.

## Results and discussion

The results are related to the performance, combustion and emission characteristics of a DI diesel engine fuelled with diesel, EPO and MPO. The performance parameters such as variation of brake thermal efficiency (BTE) and brake specific energy consumptions (BSEC) against brake mean effective pressure (BMEP) of the different fuel operations are presented in the subsequent “[Performance characteristics](#)” sections. Further, combustion characteristics such as variation of heat release rate (HRR) against crank angle (CA), ignition delay and cylinder peak pressure against BMEP are presented in “[Combustion characteristics](#)” section. The nitric oxide (NO), unburnt hydrocarbon (UBHC), carbon monoxide (CO) and smoke emissions against BMEP were measured and compared with diesel fuel in “[Exhaust emissions characteristics](#)” section.

## Performance characteristics

### Comparison of brake thermal efficiency for various fuels

Figure 7 shows a comparison of the brake thermal efficiency with respect to BMEP for the different pyrolysis waste engine

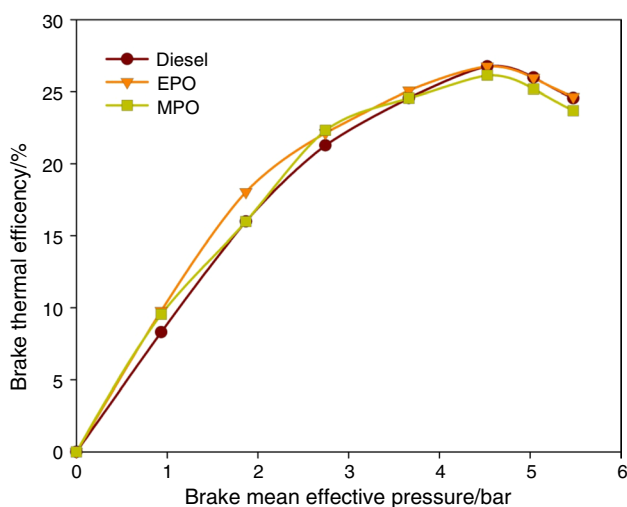


**Table 7** Uncertainties of engine measuring parameters

Instrument	Measuring range	Resolution/accuracy	Calibrated percentage uncertainties
<i>AVL DiTEST gas 1000 BL analyser</i>			
Carbon monoxide (CO)	0–10 vol%	0.01 vol%	±0.2
Carbon dioxide (CO <sub>2</sub> )	0–20 vol%	0.1 vol%	±0.15
Unburned hydrocarbon (UBHC)	0–20,000 ppm	2 ppm	±0.2
Nitric oxide (NO)	0–5000 ppm	1 ppm	±0.2
AVL 415SE smoke meter	0–10 FSN	0.001 FSN	±1
Crank angle encoder	–	±1°	±0.2
Pressure transducer	0–100 bar	±0.01 bar	±0.1
Speed	0–5000 rpm	–	±0.5%
Load	12 kg	±0.1 kg	±0.5%

**Table 8** Uncertainty of engine performance and emission parameter

S. no.	Engine characteristics	Expanded uncertainties	Experimental percentage uncertainties
1	Brake power	±0.0854 kW	±3.56
2	Total fuel consumption	±0.01033 kg h <sup>-1</sup>	±1.2
3	Brake specific fuel consumption	±0.0030 kg kWh <sup>-1</sup>	±0.622
4	Brake specific energy consumption	±0.86 kJ kWh <sup>-1</sup>	±1.83
5	Carbon monoxide	±0.075 vol%	±5.2
6	Hydrocarbon	±3 ppm	±7.9
7	Nitric oxide	±9 ppm	±1.1
8	Smoke emission	±0.041 FSN	±2.2

**Fig. 7** Brake thermal efficiency for various fuels with BMEP

oils. The BTE of diesel and both pyrolysis oils show similar trends compared with each other. The BTE obtained for diesel fuel at rated load was 26%, whereas it was 25.19% for MPO and 25.95% for EPO. BTE attained for EPO was closer to diesel value at rated load due to similar viscosity. The BTE

obtained for EPO and MPO was slightly higher than diesel at partial loading conditions. This might be due to their higher calorific value of the EPO and MPO compared to standard diesel fuel. The average BTE of EPO and MPO was 1% and 1.5% higher than diesel at partial loading conditions, respectively. The BTE of the pyrolysis fuel was higher up to 80% of the load. MPO has higher ignition delay, poor volatility and higher viscosity which affected the atomisation and fuel evaporation, resulting in slower combustion. Also, fuel quantity is injected into the engine cylinder at a rated load taking higher time to evaporate [39]. This leads to a decrease in BTE for MPO at rated load condition, which was also slightly lower than both diesel and EPO. Thus, combustion was incomplete while MPO was used as a sole fuel which led to a decrease in BTE.

#### Comparison of brake specific energy consumption for various fuels

The brake specific energy consumption for the EPO and MPO were almost followed similar trends as the diesel as shown in Fig. 8. During rated load conditions, the BSEC obtained for diesel was 13.69 MJ kWh<sup>-1</sup>. Similarly, both pyrolysis oils showed similar values of BSEC compared

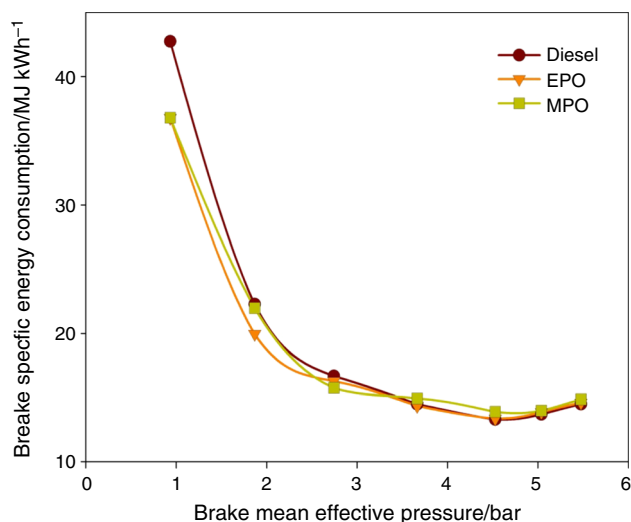


**Fig. 8** Brake specific energy consumption for various fuels with BMEP

with diesel at rated load conditions. The MPO has obtained  $13.98 \text{ MJ kWh}^{-1}$ , which was slightly higher than that of diesel and EPO at rated load. At partial load conditions, the BSEC of diesel was higher than that of both pyrolysis oils. The BSEC of diesel at 40% loading was  $16.66 \text{ MJ kWh}^{-1}$ , which was 2.4% and 5.5% higher than that of EPO and MPO, respectively. Specific energy consumptions of EPO and MPO were 1.4% and 2.11% higher than that of diesel at rated load condition because of its higher calorific value in pyrolysis oils when compared to diesel. The BSEC for MPO at rated load conditions was higher than that of diesel and EPO due to higher viscosity, also the presence of trace amount of alcohol and other constituents in MPO which undergoes delayed combustion, which causes power loss and incomplete combustion [40]. Higher viscosity and higher ignition delay affects the combustion and decrease the power output, resulting in a higher amount of fuel consumption to attain the required amount of power.

## Combustion characteristics

### Comparison of heat release rate for various fuels

The heat release rate for EPO, MPO and diesel fuel at rated load condition is shown in Fig. 9. It was observed that EPO has a higher heat release rate compared to diesel and MPO at the premixed stage. Meanwhile, MPO has a higher heat release rate compared to other fuels in the controlled combustion phase. The heat release rate is majorly affected by calorific value, viscosity and ignition delay. The premixed heat release rate was maximum for EPO which is  $74.18 \text{ J deg}^{-1} \text{ CA}^{-1}$ , occurring at  $1^\circ$ —crank angle, whereas

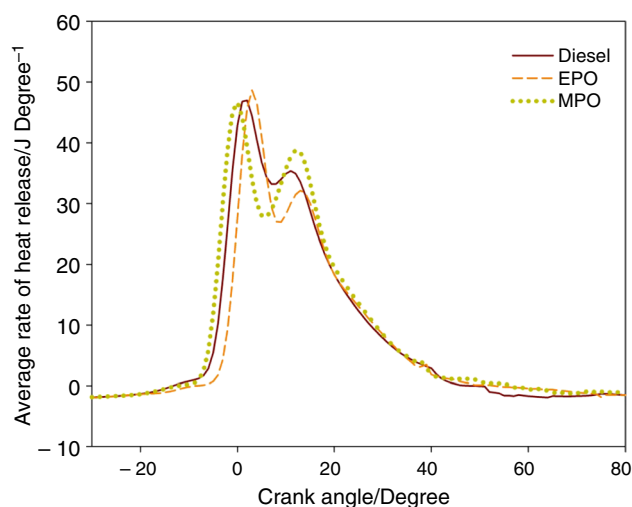


**Fig. 9** Heat release rate for various fuels with crank angle at full load

diesel has the maximum heat release rate of  $59.92 \text{ J deg}^{-1} \text{ CA}^{-1}$ , occurring at  $3^\circ$ —crank angle. Similarly, the maximum premixed heat release rate of MPO was  $48.64 \text{ J deg}^{-1} \text{ CA}^{-1}$ , occurring at  $3^\circ$ —crank angle. In the diffused phase, the maximum heat release rate was derived as  $35.34$ ,  $32.82$  and  $38.84 \text{ J deg}^{-1} \text{ CA}^{-1}$  for diesel, EPO and MPO, respectively. Generally, low ignition delay results in the minimum heat release rate in the premixed stage. However, EPO has a higher calorific value and higher viscosity when compared to diesel; therefore, a higher heat release rate was obtained in contrast to the general trend. It is also observed that the heat release rate for MPO was higher than diesel at diffused combustion phase. Influence of higher viscosity and ignition delay of MPO reduces the heat release rate in the premixed combustion, although it has higher calorific value than EPO. The maximum heat release rate of MPO was shifted to the diffused phase because of poor atomisation due to higher viscosity and chemical ignition delay. The presence of alcohol and other constituents increases the ignition delay of MPO. Higher ignition delay and slower combustion result in low charge temperature in the premixed stage, which leads to minimum heat release rate for the MPO [41].

### Comparison of ignition delay for various fuels

Figure 10 shows the ignition delay of diesel and different pyrolysis oils is plotted against BMEP. The ignition delay decreases with increasing the load for all fuels. It was observed that the ignition delay of EPO was lower than that of diesel and MPO. The MPO showed the maximum ignition delay at all the loading conditions. The ignition delay of diesel is  $14^\circ$ —crank angle at rated load and it lies in between the ignition delay of MPO and EPO for all loading conditions. The ignition delay of MPO was longer than diesel by

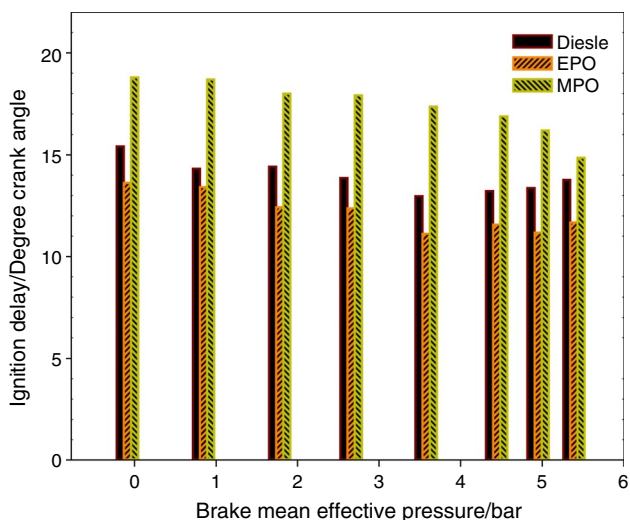


Fig. 10 Ignition delay for various fuels with BMEP

approximately 4°—crank angle. The ignition delay for EPO is shorter than diesel by approximately about 3°—crank angle. The negligible amount of sulphur present in both PO causing lower ignition delay, nevertheless, due to the presence of alcohol traces and higher viscosity of MPO increases the physical and chemical ignition delay. All hydrogen-enriched fuels show long ignition delay due to the higher auto-ignition temperature of hydrogen [38]. MPO contains more hydrogen contents than EPO and diesel, which results in longer ignition delay.

**Comparison of cylinder peak pressure for various fuels**

Figure 11 shows the deviation of cylinder peak pressure for various fuels with BMEP. Cylinder peak pressure increases

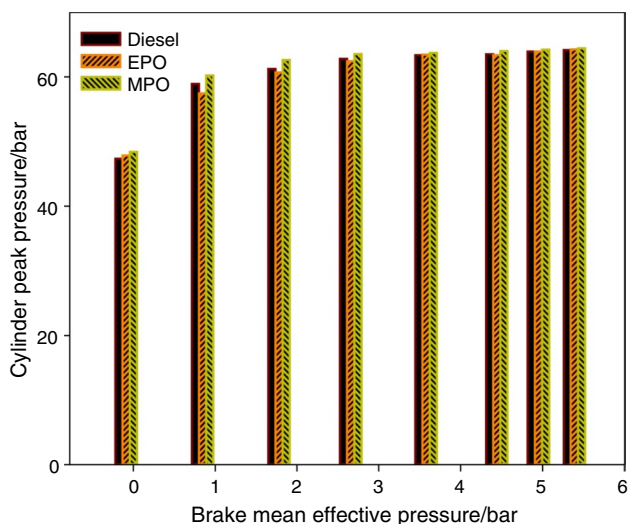


Fig. 11 Cylinder peak pressure for various fuels with BMEP

gradually with an increase in load. The peak pressures attained by different fuels are identical at higher loads. The peak pressure attained by EPO was comparatively equal to the peak pressure of diesel when tested under partial load conditions. The peak pressure recorded by MPO was invariably higher when compared to the peak pressure of diesel at partial load. Under the no-load conditions, the peak pressure of 47.36, 48.87 and 48.43 bar were attained for diesel, EPO and MPO, respectively, whereas the peak pressure of 63.93, 63.92 and 64.23 bar were attained for the diesel, EPO and MPO under rated load conditions, respectively. In the starting stage, the peak pressure is governed by the combustion rate and delay period, which is influenced by the amount of fuel consumed in the premixed combustion phase. MPO has a slower combustion rate due to higher viscosity and longer ignition delay, which are the main factors for higher peak pressure.

**Exhaust emissions characteristics**

**Comparison of nitric oxide emissions for various fuels**

NO formation in CI engines depends upon the maximum combustion temperature, residence time and oxygen concentration. NO emission increases with an increase in load and combustion temperature. Figure 12 shows that NO emission for diesel fuel was 1030 ppm at rated load, whereas NO emissions of EPO and MPO were 749 ppm and 892 ppm, respectively. At rated load, nitric oxides emission in EPO and MPO were 27% and 13% lower than diesel, respectively. NO emissions of EPO were lower as compared to diesel and MPO at all loading conditions. NO emission of diesel, EPO and MPO at 110% loads was observed as 968, 734 and 875 ppm, respectively. Higher hydrogen to oxygen

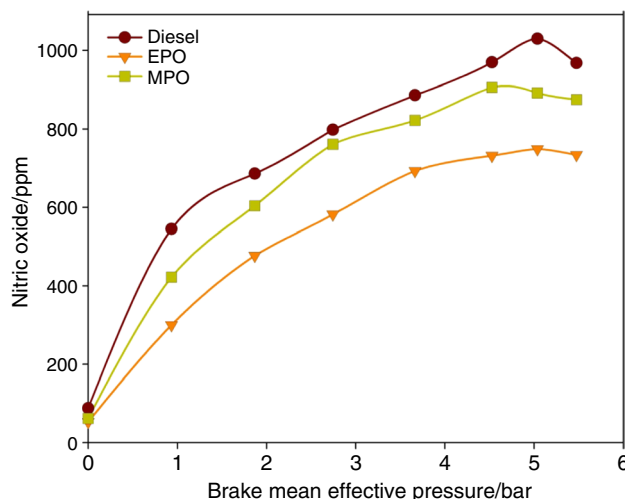


Fig. 12 Nitric oxide for various fuels with BMEP

ratio present in both EPO and MPO results in the formation of water vapour during the combustion process. The presence of higher water content in the cylinder leads to lower combustion temperature and an increase in the specific heat capacity of the gas, which results in lower NO emissions. However, for MPO, the formation of water vapour is very less even though it has higher hydrogen percentage causing higher NO emission than EPO. This is due to the incomplete combustion of the fuel. The higher ignition delay and lower heat release rate in the premixed combustion stage are primary reasons for less NO formation in MPO compared to diesel [42].

### Comparison of unburnt hydrocarbon emissions for various fuels

Figure 13 shows that unburnt hydrocarbon emission (UBHC) of MPO was higher when compared to diesel and EPO under rated load conditions. At rated load, the maximum UBHC emission of MPO was 70 ppm, whereas UBHC of EPO and diesel were 65 ppm and 61 ppm, respectively. UBHC emission of MPO was 14.7% and 6.5% higher than that of diesel and EPO, respectively. At no-load condition, UBHC of diesel, EPO and MPO were 22, 22 and 26 ppm, respectively. Similarly, UBHC of 44, 49 and 54 ppm was obtained at partial loading conditions. The presence of alcohol in MPO leads to quenching of combustion reactions and resulting in low combustion temperature. These regions will cause intermediate species like formaldehyde and alkenes to be emitted which form UBHC. Due to higher viscosity and density of MPO causes poor atomisation in the combustion chamber. Poor atomisation increases the ignition delay of the fuel and exhibits the slow combustion of MPO, which enhances the diffusion combustion phase. In this diffusion phase, the fuel

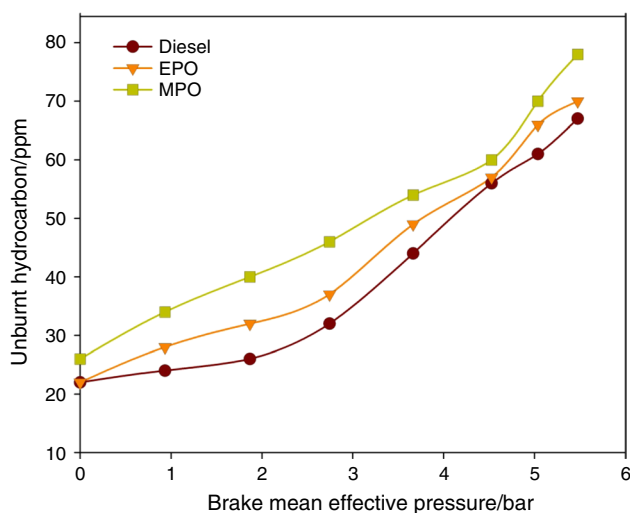


Fig. 13 Unburnt hydrocarbon for various fuels with BMEP

mixes with air during expansion resulting in delayed combustion leading to UBHC emissions [37].

### Comparison of carbon monoxide emissions for various fuels

Incomplete combustion of fuel in the engine cylinders is the primary source of CO emissions. During combustion, fuel was first converted into low molecular weight hydrocarbons (including olefins and aromatics) and then converted into aldehydes, ketones and CO. In the end, CO gets oxidised and converted into CO<sub>2</sub>. This CO to CO<sub>2</sub> conversion step is slow when compared with that of hydrocarbon to CO conversion. Incomplete conversion of CO to CO<sub>2</sub> occurred because of the lower amount of oxygen in the combustion chamber; thus, CO does not get enough time to oxidise. Figure 14 shows that CO emissions increase with the increase in load for all the fuels. CO emissions for MPO and EPO were higher, compared to that of diesel at all loaded conditions. At rated load, the CO emissions for MPO, EPO and diesel were 0.8%, 0.78%, and 0.62%, respectively. At rated load, the CO emissions of diesel were 25% and 29% lower than EPO and MPO, respectively, and CO emission was nearly constant up to 60% load and started increasing above 60% load. CO emissions of diesel, EPO and MPO were 0.38%, 0.55% and 0.57% at 80% of the rated load. CO emission was lesser in the diesel combustion cycle due to excess air. As the viscosity of MPO was higher when compared to that of diesel fuel resulted in poor atomisation; also, the air–fuel mixture is very lean at the wall and crevice volume of the cylinder. The rich core and the lean crevice volume results in poor flame propagation, leading to incomplete combustion of MPO. Besides, the fuel consumptions of MPO and EPO are higher when compared to that of diesel; hence, decrease in air–fuel ratio causes higher CO emission.

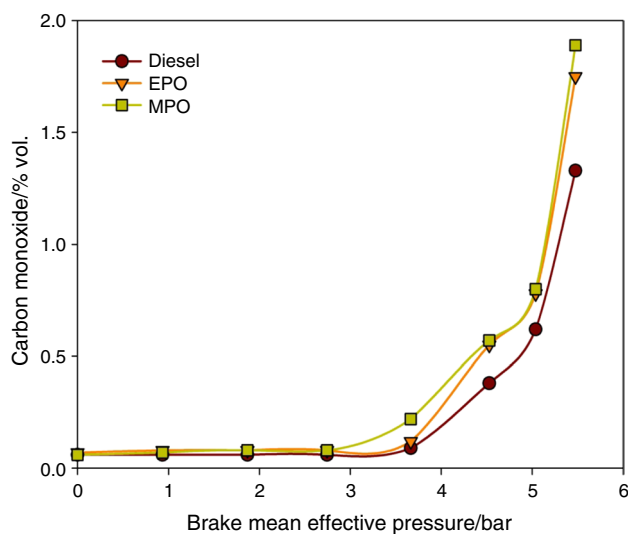


Fig. 14 Carbon monoxide emission for various fuels with BMEP



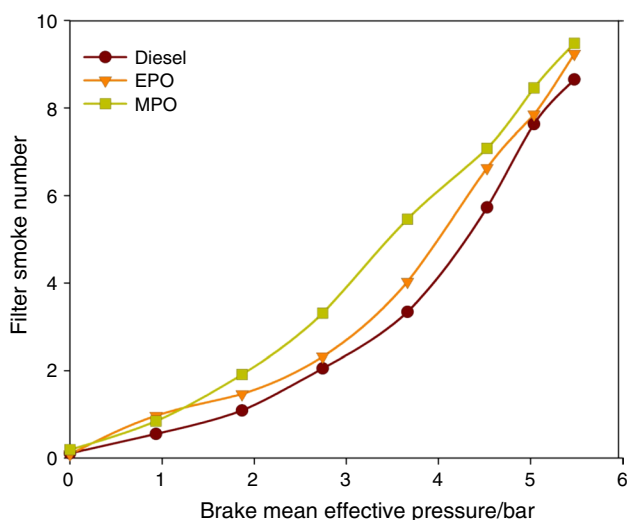


Fig. 15 Smoke emission for various fuels with BMEP

**Comparison of smoke emissions for various fuels**

Figure 15 shows that a comparison of smoke emission for diesel, EPO and MPO at various loads. Smoke increases with increase in engine load. At the rated load, FSN for MPO was the highest, which is 8.4 and for EPO and diesel were measured as 7.85 and 7.63, respectively. At no-load condition, FSN value was measured as 0.106, 0.085 and 0.195 for diesel, EPO and MPO, respectively. Smoke emissions of EPO and MPO were 2.8% and 10% higher than that of diesel at rated load conditions. Smoke is a collection of solid carbon soot particles coming out from the exhaust gas. Higher FSN value shows the presence of more amount of soot formation during the combustion. From the graph, it is observed that MPO has higher FSN compared with both diesel and EPO at all the loading conditions. During pyrolysis, lightweight carbon and other low boiled materials are evaporated and form particulate matters on the pyrolysis fuel. These particles are the ones converted into soot during the diffusion combustion phase. The combustion rate of MPO was much slower compared to both EPO and diesel resulting in higher smoke emission.

**Energy and exergy analysis**

The maximum possible useful energy from the system and the process is mentioned in terms of exergy. Exergy is used to improve the process efficiency to attain the maximum efficiency of the engine operation with engine modification or fuel modification. In this proposed work, the exergy analysis used to measure the theoretical performance of EPO and MPO and its energy losses for a better assessment to reduce the possible energy loss. An energy analysis of

engine provides maximum work done and heat transfer by the exhaust gas, cooling water and unaccounted losses to optimise the energy distribution. Also, exergy efficiency can be calculated based on the energy analysis to find the effectiveness of the system. The second law of efficiency, which is known as exergy efficiency is calculated by the ratio of exergy utilised by the system to the total exergy input from the fuel combustion. The exergy utilised by the system includes exergy on the shaft power, exergy on the cooling water heat loss and exhaust heat loss [43]. The energy and exergy analysis of EPO and MPO were determined and compared to each other.

**Energy balance**

Energy analysis was carried out using the following equations. It represents how much energy transferred from the fuel to the various sources and losses.

The energy supplied from the fuel can be measured by the calorific value it represents in Eq. (3)

$$Q_{in} = m_f \times LHV \tag{3}$$

The energy transferred to the output shaft power can be calculated by Eq. (4)

$$Q_s = \frac{(2 \times \pi \times N \times T)}{60 \times 1000} \tag{4}$$

The energy transferred to the cooling water per unit time is mentioned in Eq. (5)

$$Q_w = m_w \times Cp_w \times (Tc_2 - Tc_1) \tag{5}$$

The energy transferred to exhaust gas per unit time is represented in Eq. (6)

$$Q_e = (m_a + m_f) \times Cp_e \times (Te_2 - Te_1) \tag{6}$$

Note:  $Cp_e$  can be found by equating  $Q_w$  and  $Q_e$ .

Unaccounted energy losses per unit time are represented in Eq. (7)

$$Q_u = Q_{in} - (Q_s + Q_w + Q_e) \tag{7}$$

where  $Q_{in}$ ,  $Q_s$ ,  $Q_w$ ,  $Q_e$  and  $Q_u$  are energy transfer from fuel and energy transferred to the shaft, cooling water, exhaust gas and unaccounted losses. LHV represent the lower calorific value of fuel,  $N$  and  $T$  represent speed and torque of the engine,  $m_w$ ,  $m_a$  and  $m_f$  represent mass flow rate of water, air and fuel.  $Cp_w$  and  $Cp_e$  represent specific heat of the water and exhaust gas and  $Tc_2$ ,  $Te_2$  and  $Tc_1$ ,  $Te_1$  represent outlet and inlet temperature of cooling water and exhaust gas, respectively.

## Exergy balance

The theoretical maximum energy changes can be calculated using the following equations in the thermodynamic process [43].

The availability of fuel energy ( $A_{in}$ ) is calculated using Eq. (8)

$$A_{in} = m_f \times LHV_f \times \{1.0401 + 0.1728(H/C) + 0.0432(O/C) + 0.2169(S/C) \times (1 - 2.0268(H/C))\} \quad (8)$$

where H, C, O and S are the elemental composition of hydrogen, carbon, oxygen and sulphur in mass fraction.

Availability in output shaft work is calculated using Eq. (9)

$$A_s = \text{Brake power of the engine} \quad (9)$$

Availability of energy transferred in cooling water is calculated using Eq. (10)

$$A_w = Q_w - [m_w \times C_{p_w} \times T_a \times \ln(T_{c_2}/T_{c_1})] \quad (10)$$

where  $T_a$  is ambient temperature.

Availability of exhaust gas is calculated using Eq. (11)

$$A_e = Q_e + \left[ (m_a + m_f) \times T_a \times \{C_{p_e} \times \ln(T_a/T_{e_2})\} - \left( Re * \ln\left(\frac{p_a}{p_e}\right) \right) \right] \quad (11)$$

where  $p_a$  and  $p_e$  represent ambient and exhaust gas pressure.

Destructed availability is calculated using Eq. (12)

$$A_d = A_{in} - (A_s + A_w + A_e) \quad (12)$$

Second law efficiency or exergy efficiency can be expressed in Eq. (13)

$$\eta_{II} = 1 - (A_d/A_{in})\% \quad (13)$$

Entropy generation can be mentioned in Eq. (14)

$$S = \frac{A_d}{T_{amb}} \text{ kW/K} \quad (14)$$

Figure 16 exhibits the energy and exergy variation of EPO and MPO under different loading conditions. In energy analysis, MPO was capable of supplying higher input heat due to higher calorific value and fuel consumption. Cooling water energy loss was maintained 20–24% in EPO, which was 3% higher than that of MPO combustion. Exhaust gas energy loss of MPO was 2% higher than that of EPO due to delay in the combustion of MPO under all loading conditions. In both energy and exergy analysis, shaft power was increased with an increase in the load. EPO has higher shaft

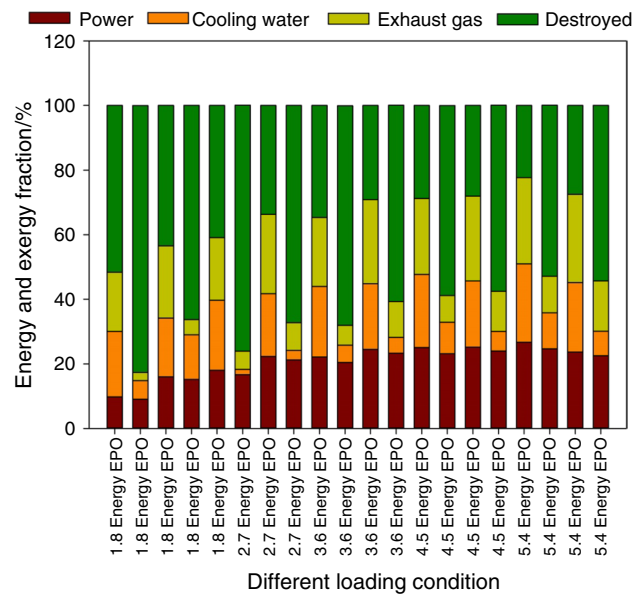
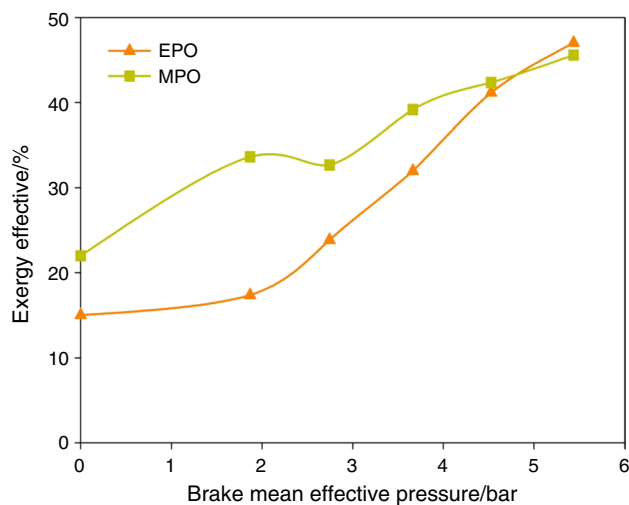


Fig. 16 Energy and exergy variation of EPO and MPO

power when compared to MPO due to effective and complete combustion, although the shaft power availability percentage of MPO was slightly higher than that of EPO, which indicates that reduced heat transfer availability loss. Moreover, higher H/C ratio of MPO decreases the fuel chemical availability on mass basis, which causes higher shaft availability. At higher loads, shaft availability of MPO was decreased due to improper combustion and higher fuel consumption. Similarly, availability destroyed in MPO which was lower than EPO except for rated load condition. The destruction availability of MPO was varied from 66 to 54% from low load to full load condition; however, in EPO destruction availability varied from 82 to 52%.

The exergy efficiency was increased with increasing load for both EPO and MPO. The higher exergy efficiency was attained in MPO compared to EPO up to the rated load condition. Figure 17 illustrates the variation of exergy efficiency with respect to BMEP. The second law efficiency of MPO varied from 33 to 45% at low load to rated load condition. Similarly, the second law efficiency of EPO varied from 17 to 47%. Decrease in fuel availability and heat transfer losses increase the exergy efficiency of MPO. Also, entropy generation was higher in EPO operation due to higher cylinder temperature. The maximum and minimum entropy generation of EPO has been calculated as  $0.017 \text{ kJ kg}^{-1} \text{ K}^{-1}$  and  $0.026 \text{ kJ kg}^{-1} \text{ K}^{-1}$  at partial and rated loads, respectively. In the case of MPO, the minimum and maximum entropy generations were  $0.013 \text{ kJ kg}^{-1} \text{ K}^{-1}$  and  $0.028 \text{ kJ kg}^{-1} \text{ K}^{-1}$ , respectively. Thus, when compared to EPO, MPO has a higher potential to use alternative fuel. Delayed combustion of MPO leads to an increase in exhaust heat loss and the



**Fig. 17** Exergy efficiency of EPO and MPO

availability of exhaust gas due to the increase in exhaust gas temperature. Cooling water heat lost and the availability of cooling water is decreased in MPO due to lower in-cylinder temperature. Hence, proper modification and improvement in the combustion are necessary to attain the maximum possible efficiency of the MPO.

## Conclusions

The physicochemical properties of electrical and microwave pyrolysis oils were found and compared with each other. Also, major properties of EPO such as calorific value, viscosity, copper strip corruptions were compared with the previous study and found to be the same. Scale-up the electrical pyrolysis reactor only influences the pyrolysis oil yield. The pyrolysis oil yield was 4% higher in electrical pyrolysis compared to the small-scale reactor, which is mentioned in an earlier publication [3]. Also, the pyrolysis oil yield was 8% higher in electrical pyrolysis when compared with microwave pyrolysis. Higher calorific value and higher H/C ratio were obtained in the microwave pyrolysis as an advantage. Further, the following conclusions are drawn from the results obtained by different pyrolysis oil used for the engine study.

- MPO has lower brake thermal efficiency at rated load compare to both diesel and EPO, while EPO and diesel have nearly the same efficiency. MPO has an efficiency of 25% at rated load, whereas diesel and EPO both have 26%.
- The specific energy consumptions of EPO and MPO were 1.4% and 2.11% higher than that of diesel at rated load conditions. However, at partial loading conditions, EPO and MPO have lower specific fuel consumption compared to diesel because of its higher calorific value.

- At the rated load, EPO has lower ignition delay than diesel by  $3^\circ$ —crank angle and MPO has higher ignition delay than diesel fuel by  $4^\circ$ —crank angle.
- The heat release rate of EPO was higher than that of premixed stages, such as  $74.18 \text{ J deg}^{-1} \text{ CA}^{-1}$ , which was 30% higher than that of diesel and 50% higher than MPO at the same stage. This is because of higher calorific value. The MPO has a higher heat release rate than that of EPO and diesel at only in controlled combustion because of its slow combustion.
- At rated load, nitric oxides emissions in EPO and MPO were 27% and 13% lower than diesel fuel, respectively.
- Carbon monoxide emissions in EPO and MPO were 25% and 29% higher than that of diesel fuel, respectively, at rated load conditions.
- UBHC emissions in EPO and MPO were higher than that of diesel fuel by 6.5% and 14.7%, respectively. Similarly, the FSN value of EPO and MPO were 2.8% and 10% higher than that of diesel at rated load.
- Exergy analysis shows that MPO has higher exergy efficiency compared to EPO due to higher calorific value.

From this work, the performance, combustion and emission characteristics of EPO were more superior to MPO due to similar physicochemical characteristics of EPO and diesel. Therefore, a further research study will be needed to improve the microwave pyrolysis oil quality and combustion efficiency. Different kinds of additives and surfactants such as diethyl ether and 1,4-dioxane mentioned in Table 1 may increase the combustion efficiency of the MPO. Hence, this work could be extended in the future using engine modification and fuel modification for the use of MPO in the CI engine.

**Acknowledgements** The authors would like to acknowledge the Department of science and technology—Science and Engineering Research Board (DST-SERB) for providing funding to carry out the research project (Project No. DST/SB/EMEQ-251). Also, the authors acknowledge the Director, National Institute of Technology, Tiruchirappalli, Tamil Nadu, India, for supporting and extending the facility to the successful completion of this research work.

## References

1. Cormier SA, Lomnicki S, Backes W, Dellinger B. Origin and health impacts of emissions of toxic by-products and fine particles from combustion and thermal treatment of hazardous wastes and materials. *Environ Health Perspect*. 2006;114:810–7.
2. Lam SS, Chase HA. A review on waste to energy processes using microwave pyrolysis. *Energies*. 2012;5:4209–32.
3. Santhoshkumar A, Anand R. Microwave-assisted fast pyrolysis of hazardous waste engine oil into green fuels. In: Kalam A (ed) *Advances in eco-fuels for a sustainable environment*. 2019, pp 119–55.

4. Lam SS, Russell AD, Chase HA. Pyrolysis using microwave heating: a sustainable process for recycling used car engine oil. *Ind Eng Chem Res.* 2010;49:10845–51.
5. Gómez-Rico MF, Martín-Gullón I, Fullana A, Conesa JA, Font R. Pyrolysis and combustion kinetics and emissions of waste lube oils. *J Anal Appl Pyrolysis.* 2003;68–69:527–46.
6. Lalvani JIJR, Parthasarathy M, Dhinesh B, Annamalai K. Pooled effect of injection pressure and turbulence inducer piston on performance, combustion, and emission characteristics of a DI diesel engine powered with biodiesel blend. *Ecotoxicol Environ Saf.* 2016;134:336–43.
7. Thiyagarajan S, Sonthalia A, Edwin Geo V, Prakash T, Karthickeyan V, Ashok B, et al. Effect of manifold injection of methanol/n-pentanol in safflower biodiesel fuelled CI engine. *Fuel.* 2020;261:116378.
8. Mohan D, Pittman CU, Steele PH. Pyrolysis of wood/biomass for bio-oil: a critical review. *Energy Fuels.* 2006;20:848–89.
9. Lam SS, Russell AD, Chase HA. Microwave pyrolysis, a novel process for recycling waste automotive engine oil. *Energy.* 2010;35:2985–91. <https://doi.org/10.1016/j.energy.2010.03.033>.
10. Sharma BK, Moser BR, Vermillion KE, Doll KM, Rajagopalan N. Production, characterization and fuel properties of alternative diesel fuel from pyrolysis of waste plastic grocery bags. *Fuel Process Technol.* 2014;122:79–90. <https://doi.org/10.1016/j.fuproc.2014.01.019>.
11. Huang YF, Te Chiueh P, Lo SL. A review on microwave pyrolysis of lignocellulosic biomass. *Sustain Environ Res.* 2016;26:103–9.
12. Wang XH, Chen HP, Ding XJ, Yang HP, Zhang SH, Shen YQ. Properties of gas and char from microwave pyrolysis of pine sawdust. *BioResources.* 2009;4:946–59.
13. Onay O, Kockar OM. Slow, fast and flash pyrolysis of rapeseed. *Renew Energy.* 2003;28:2417–33.
14. Tripathi AK, Ojha DK, Vinu R. Selective production of valuable hydrocarbons from waste motorbike engine oils via catalytic fast pyrolysis using zeolites. *J Anal Appl Pyrolysis.* 2015;114:281–92.
15. Liu WJ, Tian K, Jiang H, Zhang XS, Ding HS, Yu HQ. Selectively improving the bio-oil quality by catalytic fast pyrolysis of heavy-metal-polluted biomass: take copper (Cu) as an example. *Environ Sci Technol.* 2012;46:7849–56.
16. Lam SS, Liew RK, Cheng CK, Chase HA. Catalytic microwave pyrolysis of waste engine oil using metallic pyrolysis char. *Appl Catal B Environ.* 2015;176–177:601–17. <https://doi.org/10.1016/j.apcatb.2015.04.014>.
17. Domínguez A, Menéndez JA, Inguanzo M, Bernad PL, Pis JJ. Gas chromatographic-mass spectrometric study of the oil fractions produced by microwave-assisted pyrolysis of different sewage sludges. *J Chromatogr A.* 2003;1012:193–206.
18. Yin C. Microwave-assisted pyrolysis of biomass for liquid bio-fuels production. *Bioresour Technol.* 2012;120:273–84.
19. Hussain Z, Khan KM, Hussain K. Microwave-metal interaction pyrolysis of polystyrene. *J Anal Appl Pyrolysis.* 2010;89:39–43.
20. Zhang Y, Chen P, Liu S, Peng P, Min M, Cheng Y, et al. Effects of feedstock characteristics on microwave-assisted pyrolysis—a review. *Bioresour Technol.* 2017;230:143–51.
21. Lam SS, Wan Mahari WA, Jusoh A, Chong CT, Lee CL, Chase HA. Pyrolysis using microwave absorbents as reaction bed: an improved approach to transform used frying oil into biofuel product with desirable properties. *J Clean Prod.* 2017;147:263–72.
22. Suriapparao DV, Vinu R. Resource recovery from synthetic polymers via microwave pyrolysis using different susceptors. *J Anal Appl Pyrolysis.* 2015;113:701–12. <https://doi.org/10.1016/j.jaap.2015.04.021>.
23. Salema AA, Ani FN. Microwave-assisted pyrolysis of oil palm shell biomass using an overhead stirrer. *J Anal Appl Pyrolysis.* 2012;96:162–72. <https://doi.org/10.1016/j.jaap.2012.03.018>.
24. Ramanathan A, Santhoshkumar A. Feasibility analysis of pyrolysis waste engine oil in CRDI diesel engine. *Energy Procedia.* 2019;158:755–60.
25. Thiyagarajan S, Sonthalia A, Edwin Geo V, Ashok B, Nanthagopal K, Karthickeyan V, et al. Effect of electromagnet-based fuel-reforming system on high-viscous and low-viscous bio-fuel fueled in heavy-duty CI engine. *J Therm Anal Calorim.* 2019;138:633–44.
26. Elumalai PV, Annamalai K, Dhinesh B. Effects of thermal barrier coating on the performance, combustion and emission of DI diesel engine powered by biofuel oil–water emulsion. *J Therm Anal Calorim.* 2019;137:593–605.
27. Kalargaris I, Tian G, Gu S. Combustion, performance and emission analysis of a DI diesel engine using plastic pyrolysis oil. *Fuel Process Technol.* 2017;157:108–15. <https://doi.org/10.1016/j.fuproc.2016.11.016>.
28. Vigneswaran R, Annamalai K, Dhinesh B, Krishnamoorthy R. Experimental investigation of unmodified diesel engine performance, combustion and emission with multipurpose additive along with water-in-diesel emulsion fuel. *Energy Convers Manag.* 2018;172:370–80.
29. Vedharaj S, Vallinayagam R, Yang WM, Chou SK, Lee PS. Effect of adding 1,4-Dioxane with kapok biodiesel on the characteristics of a diesel engine. *Appl Energy.* 2014;136:1166–73.
30. Nanthagopal K, Ashok B, Garnepudi RS, Tarun KR, Dhinesh B. Investigation on diethyl ether as an additive with calophyllum inophyllum biodiesel for CI engine application. *Energy Convers Manag.* 2019;179:104–13.
31. Arpa O, Yumrutas R, Demirbas A. Production of diesel-like fuel from waste engine oil by pyrolytic distillation. *Appl Energy.* 2010;87:122–7. <https://doi.org/10.1016/j.apenergy.2009.05.042>.
32. Beg RA, Sarker MRI, Pervez MR. Production of diesel fuel from used engine oil. *Int J Mech Mech Eng.* 2010;10:1–6.
33. Arpa O, Yumrutas R, Argunhan Z. Experimental investigation of the effects of diesel-like fuel obtained from waste lubrication oil on engine performance and exhaust emission. *Fuel Process Technol.* 2010;91:1241–9.
34. Arpa O, Yumrutas R, Alma MH. Effects of turpentine and gasoline-like fuel obtained from waste lubrication oil on engine performance and exhaust emission. *Energy.* 2010;35:3603–13. <https://doi.org/10.1016/j.energy.2010.04.050>.
35. Murugan S, Ramaswamy MC, Nagarajan G. A comparative study on the performance, emission and combustion studies of a DI diesel engine using distilled tyre pyrolysis oil–diesel blends. *Fuel.* 2008;87:2111–21.
36. Hossain AK, Davies PA. Pyrolysis liquids and gases as alternative fuels in internal combustion engines—a review. *Renew Sustain Energy Rev.* 2013;21:165–89. <https://doi.org/10.1016/j.rser.2012.12.031>.
37. Sathiyamoorthi R, Sankaranarayanan G. Effect of antioxidant additives on the performance and emission characteristics of a DICI engine using neat lemongrass oil–diesel blend. *Fuel.* 2016;174:89–96.
38. Yang Y, Brammer JG, Ouadi M, Samanya J, Hornung A, Xu HM, et al. Characterisation of waste derived intermediate pyrolysis oils for use as diesel engine fuels. *Fuel.* 2013;103:247–57.
39. Murugan S, Ramaswamy MC, Nagarajan G. Assessment of pyrolysis oil as an energy source for diesel engines. *Fuel Process Technol.* 2009;90:67–74. <https://doi.org/10.1016/j.fuproc.2008.07.017>.
40. Hürdoğan E, Ozalp C, Kara O, Ozcanli M. Experimental investigation on performance and emission characteristics of waste tyre pyrolysis oil–diesel blends in a diesel engine. *Int J Hydrogen Energy.* 2017;42:23373–8.
41. Shihadeh A, Hochgreb S. Diesel engine combustion of biomass pyrolysis oils. *Energy Fuels.* 2000;14:260–74. <https://doi.org/10.1021/ef990044x>.



42. Hossain AK, Ouadi M, Siddiqui SU, Yang Y, Brammer J, Hornung A, et al. Experimental investigation of performance, emission and combustion characteristics of an indirect injection multi-cylinder CI engine fuelled by blends of de-inking sludge pyrolysis oil with biodiesel. *Fuel*. 2013;105:135–42. <https://doi.org/10.1016/j.fuel.2012.05.007>.
43. Tamilvanan A, Balamurugan K, Vijayakumar M. Effects of nano-copper additive on performance, combustion and emission characteristics of calophyllum inophyllum biodiesel in CI engine. *J Therm Anal Calorim*. 2019;136:317–30.

**Publisher's Note** Springer Nature remains neutral with regard to jurisdictional claims in published maps and institutional affiliations.